

The Important Role of Lone-Pairs in Force Field (MM4) Calculations on Hydrogen Bonding in Alcohols

Jenn-Huei Lii and Norman L. Allinger*

Department of Chemistry, University of Georgia, Athens, Georgia 30602-2526

Received: May 23, 2008; Revised Manuscript Received: August 15, 2008

An expanded treatment of hydrogen bonding has been developed for MM4 force field calculations, which is an extension from the traditional van der Waals-electrostatic model. It adds explicit hydrogen-bond angularity by the inclusion of lone-pair directionality. The vectors that account for this directionality are placed along the hydrogen acceptor and its chemically intuitive electron pairs. No physical lone-pairs are used in the calculations. Instead, an H-bond angularity function, and a lone-pair directionality function, are incorporated into the hydrogen-bond term. The inclusion of the lone-pair directionality results in improved accuracy in hydrogen-bonded geometries and interaction energies. In this work is described hydrogen bonding in alcohols, and also in water and hydrogen fluoride dimer. The extension to other compounds such as aldehydes, ketones, amides, and so on is straightforward and will be discussed in future work. The conformational energies of ethylene glycol are discussed.

Introduction

The importance of hydrogen bonding in biological structures was realized¹ long before crystallographic structure determinations of proteins and nucleic acids were reported. The Watson–Crick² base-pair hydrogen bonding has subsequently been shown to be a feature of all known double helical structures of naturally occurring nucleic acids and is part of the basis for genetic coding in all living organisms. Although hydrogen bonds are weak as compared to covalent bonds, they are the most important forces determining the three-dimensional folding of proteins. The α -helix and the β -pleated sheet, two of the most common polypeptide structural schemes in the secondary structures of proteins,³ are stabilized by hydrogen bonding.

The relatively weak (about 3–5 kcal/mol) hydrogen bonds are of prime importance for living organisms, so much so that life as we know would be impossible without hydrogen bonds.¹ This is because many biological processes involve intermolecular recognition that has to be rapid. This recognition consequently requires a weak interaction that allows very fast association and dissociation, so that in a short time many possible combinations can be checked before the correct partners associate. Stronger interactions, with bonding energies much greater than those attained by hydrogen bonding, would seriously hinder the flow of biological information and events. For important summaries concerning hydrogen bonds, general references are available.⁴

A hydrogen bond describes the attractive force that arises between the proton donor covalent pair A–H, with its significant bond dipole, and the noncovalently bound nearest-neighbor electronegative hydrogen-acceptor atom B (Figure 1).

It is in part the Coulombic interaction of the A–H dipole with the excess electron density (or atomic dipole) at the proton-acceptor atom that forms the hydrogen-bond interaction. The strength of the hydrogen bond formed is believed to be best correlated with acidity of the hydrogen atom and basicity of

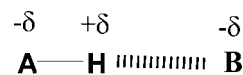


Figure 1. Classical electrostatic model for hydrogen bond.

the atom B,^{5–8} although electrostatic interactions are also important. Unless acidity of the hydrogen and basicity of the acceptor atom are sufficient, any hydrogen bonds formed are usually too weak to be significant. Of course, if the hydrogen atom is too acidic and the acceptor atom is too basic, the hydrogen will be transferred as a proton to form a covalent bond with the acceptor atom in a simple acid–base reaction.

Although the concept of a hydrogen bond has been accepted since Latimer and Rodebush⁹ published the first definitive reference on hydrogen bonding in 1920, the role of the lone-pair electrons at basic site B was not understood to be very important until 1950. Kasha^{10a} found that lone-pair electrons are affected by hydrogen bonding as observed by $n \rightarrow \pi^*$ transition shifts. Neutron and X-ray scattering experiments also show that the hydrogen-bonding hydrogens usually tend to be situated on or near the lone-pair orbital axis (B-LP).^{10b,c} In 1979, Newton et al.^{10d} applied ab initio molecular orbital calculations to the geometry of the hydrogen bonds, which further delineated the role of lone-pair in the hydrogen bonds.

Hydrogen-Bond Theory and Model

Background. Although experimental work on hydrogen bonding has been carried out for a variety of systems, many difficulties exist that often prevent the straightforward interpretation of the results. For example, vibrational spectroscopy, one of the methods most sensitive to the presence of hydrogen bonding, is often complicated by broad or overlapping bands and high degrees of association in the liquid phase. Gas-phase data are relatively sparse, difficult to obtain, and usually limited to those species having relatively strong hydrogen bonds. Furthermore, those systems that have been studied experimentally are often very complex so that measurements of hydrogen bonding must be made indirectly. Therefore, theory plays an important role in hydrogen-bonding studies.

* Corresponding author. Fax: (706) 542-2673. E-mail: allinger@chem.uga.edu.

A successful theory (or model) for the hydrogen bond has to be able to provide useful quantitative information and explain the many important properties of hydrogen-bonded complexes that are available from extensive experimental evidence. These include the following.

When the hydrogen bond, $A-H\cdots B$, is formed:

(1) The molecules concerned come much closer together than the sum of the van der Waals radii of the nearest atoms would otherwise allow.

(2) The lengths of $A-H$ bonds are somewhat increased as hydrogen-bond strength increased.

(3) As a result of (2) above, the infrared stretching frequencies of $A-H$ bonds are shifted to lower frequencies.

(4) The integrated infrared intensities of the $A-H$ stretching bands are enhanced.

(5) The polarities of the molecules concerned are increased. The dipole moment of the hydrogen-bonded complex is larger than the vectorial sum of the monomer moments.

(6) The linearity of the $A-H\cdots B$ segment tends to increase as the strength of the hydrogen bond increases.

(7) The protons of hydrogen-bond donors usually tend to be situated on or near the hybrid lone-pair orbital axes of proton acceptors.

(8) The association energy of attraction between the molecules concerned increases substantially.

Before 1957, theoretical studies of a hydrogen bond used either classical electrostatic models or approximate quantum mechanical treatments of fragments of the hydrogen-bonded system. The classical electrostatic model was the first proposed for a hydrogen bond, because of the fact that all known hydrogen bonds are between electronegative elements (A and B in Figure 1). Typical calculations utilizing this model were made by Lennard-Jones and Pople.^{11,12} With this model, the theoretical chemists successfully calculated the hydrogen-bond energy of the water dimer, $5.95 \text{ kcal mol}^{-1}$ in good agreement with the experimental values. However, the model failed to give correct predictions of hydrogen-bond lengths and other properties of hydrogen bonds, such as the increase of molecular polarity and intensity of the $A-H$ stretching frequency. The simple electrostatic model was an incomplete description of the hydrogen bond, because it did not take into account three other essential effects: polarization, delocalization, and electron exchange between bonded molecules. Therefore, a better model was needed.

A better model depended on a better understanding of the hydrogen bond. To gain such an understanding, several research groups^{13–15} tried to partition the total hydrogen-bond energy into individual contributions similar to those proposed by Coulson¹⁶ in 1957. Among them, Morokuma¹⁷ presented a more detailed scheme of energy partitioning within the framework of molecular orbital theory, which is summarized in Table 1. The energy of the hydrogen bond, ΔE_{HB} , is given by eq 1:

$$\Delta E_{\text{HB}} = \text{ES} + \text{EX} + \text{PL} + \text{CT} + \text{DISP} + \text{MIX} \quad (1)$$

where ES is the electrostatic interaction energy. This is the interaction energy between the unperturbed nuclei and electron clouds of two monomers, M_a and M_b . This contribution includes the interactions of all permanent charges and multipoles, such as charge–charge, charge–dipole, dipole–dipole, dipole–quadrupole, etc. This interaction may be either attractive or repulsive depending on the orientation of charges and multipoles. This is the dominant interaction when the two monomers are far apart.

TABLE 1: Basis Set Dependence of Energy Components (kcal/mol) for Linear $(\text{H}_2\text{O})_2$ at the Experimental Geometry^a

	STO-3G ^d	4-31G ^e	6-31G ^{*f}
EX (exchange repulsion)	4.0	4.2	4.3
ES (electrostatics)	−4.2	−8.9	−7.5
PL (polarization)	−0.1	−0.5	−0.5
CT (charge transfer)	−4.8	−2.1	−1.8
MIX	0.1	−0.3	−0.1
DE ^b	−5.1	−7.7	−5.6
monomer μ (Debye) ^c	1.72	2.6	2.2

^a This table is adapted from ref 17. Please see text for more details of definition of individual term. ^b DE is the dimerization energy. ^c Experimental value is 1.85 Debye. ^d Reference 18. ^e Reference 13. ^f Reference 15.

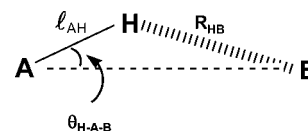


Figure 2. Geometry parameters for MM3 hydrogen-bond model.

EX is the electron exchange repulsion energy. This is the interaction energy caused by the exchange of electrons between monomers M_a and M_b . The interaction is a short-range repulsion due to the overlap of electron clouds of M_a and M_b .

PL is the polarization interaction energy. This results from the interaction between M_a and the distorted (polarized) electron cloud of M_b by M_a , or vice versa. The contribution includes charge–induced dipole, dipole–induced dipole, quadrupole–induced dipole, etc. This is always an attractive interaction.

CT is the charge transfer or electron delocalization interaction energy. It results from the interaction caused by electron transfer from the highest occupied MO (HOMO) of M_a to the lowest unoccupied MO (LUMO) of M_b , and from the HOMO of M_b to the LUMO of M_a , and higher-order coupled interactions. This interaction is always attractive and highly directional. In hydrogen-bonded structures, a net electron transfer always occurs from the molecule with the nonbonded (lone-pair) electrons, or weakly bonded (π) electrons to the molecule with a highly polarized $A-H$ bond.

DISP is the dispersion energy. This interaction is caused by simultaneous and correlated excitations of electrons in both molecules and leads to correlation of the electron motions and to general net stabilization of the complex. The correlation contribution is found to be important for interactions between nonpolar molecules, but relatively unimportant for those of small polar molecules, as in hydrogen bonding.

MIX is the sum of the higher-order interaction energies among the four ES, EX, PL, and CT components.

The results of a hydrogen-bond energy partitioning are very basis set dependent. This is clearly shown by a comparison of the results by Morokuma and Winick,¹⁸ Kollman and Allen,¹³ and Morokuma¹⁵ (see Table 1).

The numbers in this table offer some guidelines for the development of a molecular mechanics model of hydrogen bonding.

Hydrogen-Bonding Models in Molecular Mechanics. The first general and reasonably successful molecular mechanics force field developed was MM2.^{19,20} At that time, there were many more fundamental items that were of concern in molecular mechanics development, and hydrogen bonding was originally essentially bypassed in MM2. Therefore, the role of the lone-pair in hydrogen bonds was not studied, even though the lone-pair is used in the MM2 force field. We noted at the time that

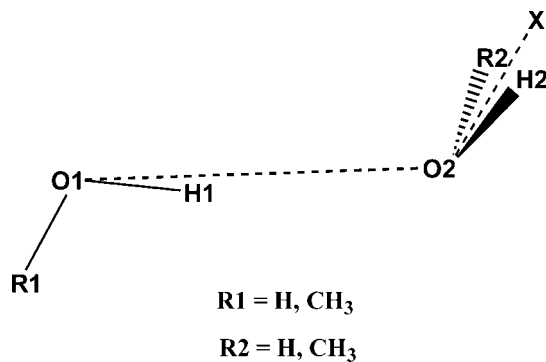


Figure 3. Water and methanol dimers.

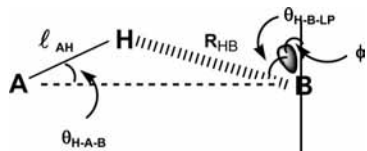


Figure 4. Geometry parameters for MM4 hydrogen-bond model.

TABLE 2: Comparison of Energy Contributions of Hydrogen-Bond Interactions Expressed in Quantum Mechanics and Molecular Mechanics

quantum mechanics	molecular mechanics
exchange repulsion (EX)	van der Waals repulsion
dispersion (DISP)	van der Waals attraction
electrostatics (ES)	charge–charge interaction
	charge–dipole interaction
	dipole–dipole interaction (either attraction or repulsion)
polarization (PL)	charge–induced dipole interaction
	dipole–induced dipole interaction (always attraction)
charge transfer (CT)	explicitly attractive hydrogen-bond term (highly directional)

hydrogen bonding had been interpreted as a largely electrostatic phenomenon, and because MM2 contained reasonable electrostatics (point charges and dipoles), it was thought (and hoped) that hydrogen bonding should be reasonably approximated without adding anything special. Indeed, as found by further studies some years later, while the original MM2 treatment of hydrogen bonding by using only the ordinary electrostatic and van der Waals terms gave qualitatively correct results, the hydrogen bonds formed in that model were quite a bit too long and too weak. Therefore, two important additions to the early hydrogen-bond treatment were added²¹ in a later version of MM2. These were corrections to the hydrogen-bond lengths, and their strengths, both of which could be rather easily taken into account. These two corrections are sizable, and they are crucial to obtain reasonable representations of hydrogen bonding in the molecular mechanics model. Quantum mechanically they result largely from the charge transfer that occurs, and they were included in MM2 in the following way. When the hydrogen and the lone-pair contributing atom (B in Figure 1) approach each other to the equilibrium distance, they come quite close together. In the original MM2 molecular mechanics, there is a large van der Waals repulsion between them. Yet in reality, because of the charge transfer, much of the repulsion is replaced by an attraction. The remaining repulsion therefore becomes dominating only at a much shorter distance. What is happening is that the repulsive part of the van der Waals curve is shifted to shorter distances, while the attraction increases because the attractive part of the curve goes downward with decreasing

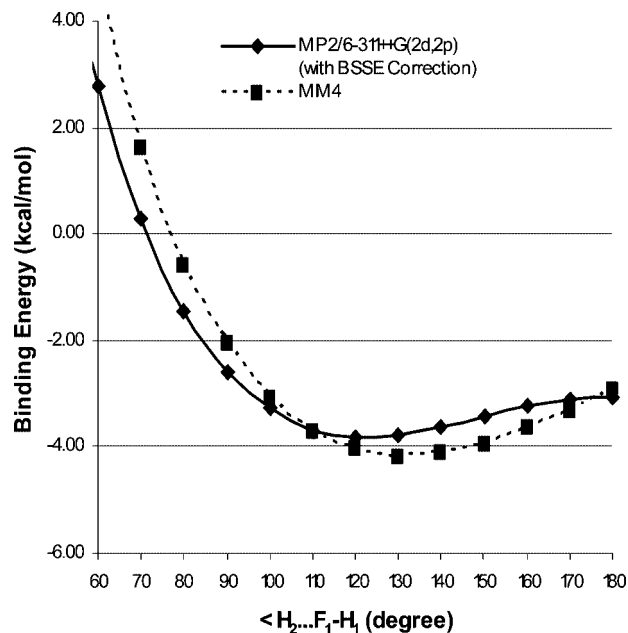


Figure 5. Hydrogen-bond energy as a function of angle for HF₂ dimer (F₁...F₂ is fixed at 2.8 Å, and ∠F₁...F₂ is fixed at 180°).

distance. This is accounted for in MM2 by a correlated change in the van der Waals parameters, in which the value for the H...B van der Waals distance (R^o) is reduced, and the depth of the well (ϵ) is increased, in such a way as to leave the normal r^{-6} attraction unchanged at longer distances. When MM3 was developed,²² the two corrections added to later versions of MM2 were carried over to it. It was found that with MM3 these two major errors in the early MM2 hydrogen bonds^{19,20} were also well corrected. The hydrogen bonds became shorter and stronger as was desired, and both of these quantities could be adequately fit simultaneously in a general way for different combinations of atom types.

While the distance and energy criteria were then reasonably well calculated for a wide variety of hydrogen bonds as above, the angular geometric quantities were still not very satisfactory. These were determined at that point solely by electrostatics and van der Waals terms. While this was sometimes adequate, it became clear that more was needed. The directionality of the hydrogen bond had another moderately strong component (charge transfer) required, generally in the direction preferred by the electrostatics.^{23,24} It also became clear that the electrostatics deduced from small basis Hartree–Fock calculations (e.g., 6-31G*) gave dipole moments for many small molecules that were in error by 15–25%.²⁵ With larger basis set calculations and some electron correlation (e.g., MP2/6-311++G(2d,2p)), the errors are smaller (but still about 15%), at least for a few well-studied classes of compounds. These errors are systematic, and thus they can be empirically corrected.²⁶

As more evidence was obtained from geometrical analysis of the hydrogen bonds observed in crystals and ab initio calculations^{10d} (as well as the unsatisfactory results for some cases in preliminary MM3 force field calculations), the importance of the angle subtended at the H atom (H-bond angularity) and the angle at the acceptor atom (lone-pair directionality) became clearer. By adding H-bond angularity to the existing MM3 hydrogen-bonding function^{23,24} (eq 2, Figure 2), a better description of hydrogen bonding was obtained (MM3(94) and later).

$$E_{\text{HB}} = \sum \varepsilon_{\text{HB}} \{184\,000 \exp[-12.0R_{\text{HB}}/R_{\text{HB}}^{\circ}] - F(\theta_{\text{H-A-B}}, I_{\text{AH}})(R_{\text{HB}}^{\circ}/R_{\text{HB}})^6\}/\text{De} \quad (2)$$

where

$$F(\theta_{\text{H-A-B}}, I_{\text{AH}}) = \cos(\theta_{\text{H-A-B}})(I_{\text{AH}}/I_{\text{OAH}})$$

and De is dielectric constant; I_{OAH} is the natural bond length of A-H; and ε_{HB} and R_{HB}° are optimum hydrogen-bonding energy and distance for $\text{H}\cdots\text{B}$, respectively.

In the MM3 molecular mechanics calculations, the hydrogen-bond energy is factored as in eq 2, and the individual terms are used in formulating the appropriate expression for the hydrogen-bond interaction. Table 2 shows the relationship between the energy components of hydrogen-bonding interaction used in quantum mechanics with those in molecular mechanics. In principle, a good force field hydrogen-bond model should give

energy partitioning that can be related to a molecular orbital calculation, at least in an approximate way.

Although the hydrogen-bond calculations were improved significantly with the inclusion of the H-bond angularity function, they still did not give accurate representations of hydrogen-bond geometries in some cases. For example, in the linear water dimer, the angle of $\text{O1}\cdots\text{O2}\cdots\text{X}$ ($\text{O2}\cdots\text{X}$ is the bisector of the H2-O2-H2 angle; see Figure 3) is calculated to be 160° with MM3, which is too big as compared to the experimental value, 123° (10), and the ab initio value, 123° . Also, the $\text{F}\cdots\text{F-H}$ angle in the hydrogen fluoride dimer is calculated to be 180° in MM3, while the experimental and ab initio values are 117° (6) and 112° , respectively. Moreover, in the ethylene glycol calculations, MM3 systematically underestimates the hydrogen-bonding energies for those conformations that have close $\text{O1}\cdots\text{O2}$ contacts and a lone-pair on one oxygen that is pointing toward the hydrogen on the other oxygen. All of these

TABLE 3: MM4 Hydrogen-Bonding Parameters^{a,b}
Hydrogen Bonding Parameters

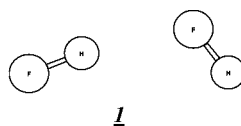
Hydrogen Bond Type	ε_{HB}	R_{HB}°
F...H(F) (11...176)	2.587	1.78
O...H(OR) (6...21)	1.700	1.88
O...H(OH) (6...180)	2.933	1.93

Bond Parameters ^c				
Bond Type	K_s	l_0	BM	BM _{induced}
F-H (11-176)	9.200	0.931	1.820	1.820

Torsional Parameters (kcal/mole) ^d					
Torsional Type	V_1	V_2	V_3	V_4	V_6
O-C-C-O (6-1-1-6)	-1.186	-0.639	1.095	0.000	-0.100

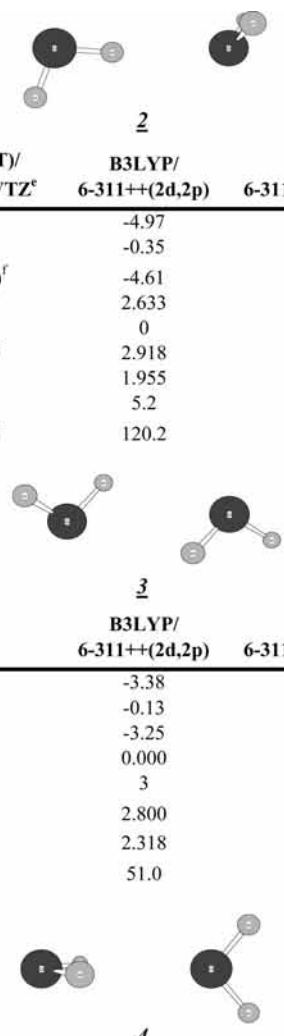
^a ε_{HB} is the well depth parameter in the hydrogen-bonding equation in kcal/mol, and R_{HB}° is the distance between the atoms at the energy minimum in angstroms. ^b All other necessary parameters, except F-H (11-176) bond and O-C-C-O (6-1-1-6) torsional parameters, are from published MM4 papers: alkanes (ref 29a) and alcohols/ethers (ref 29b-f). ^c Stretching constant (K_s) in mdyn/Å; natural bond length (l_0) in Å; bond moments (BM and BM_{induced}) in Debye. ^d New O-C-C-O torsional parameters are needed to account for the change of 6...0.21 hydrogen-bonding parameter. These torsional parameters as well as hydrogen-bonding parameters listed above will be included in the MM4(2003R4) and later.

TABLE 4: Geometry and Energy of Hydrogen Fluoride Dimer^{a,b}



Exp. ^c	CCSD(T)		B3LYP/		MP2/	
	Limit ^e	6-311++G(2d,2p)	6-311++G(2d,2p)	MM3	MM4	
I. (HF)₂ (linear, C_s), I						
E(uncorrected)			-4.79	-4.87		
BSSE			-0.38	-0.97		
E(corrected)	-4.56(28) ^d	-4.57(5)	-4.41	-3.90	-5.69	-4.55
Dipole Moment	2.988	3.32	3.414	3.569	3.640	3.179
Imaginary Fre.	0		0	0	0	0
F...F dist.	2.72(3)	2.735(10)	2.743	2.762	2.793	2.754
F...H dist.			1.826	1.846	1.873	1.832
<H-F...F	10(2)	7(1)	7.8	6.0	0	7.2
<F...F-H	117(6)	112(2)	110.0	111.5	180.0	124.8

^a Experiment geometry is microwave r_0 values; MM3 and MM4 geometries are r_g values. Energies are in kcal/mol; distances are in Å; angles are in deg. ^b All four atoms are in the same plane. ^c Reference 33a. ^d Reference 33b. ^e Reference 33c and 33d.

TABLE 5: Geometries and Energies of Water Dimers^a


I. (H ₂ O) ₂ (linear, C _s), 2						
	Exp. ^c	CCSD(T)/ aug-cc-pVTZ ^e	B3LYP/ 6-311++(2d,2p)	MP2/ 6-311++G(2d,2p)	MM3	MM4
E(uncorrected)			-4.97	-5.36		
BSSE			-0.35	-0.88		
E(corrected)	-5.4(2) ^d	-5.0(1) ^f	-4.61	-4.48	-4.77	-4.59
Dipole Moment	2.6		2.633	2.783	3.508	2.494
Imaginary Fre.	0		0	0	0	0
O...O dist.	2.976	2.895	2.918	2.917	2.942	2.956
O...H dist.			1.955	1.956	2.007	1.987
<H-O...O	6(20)	4.8	5.2	4.6	8.9	2.8
<O..O..X ^b	123(10)	122.5	120.2	123.7	160.3	123.0

II. (H ₂ O) ₂ (cyclic, C _{2h}), 3					
		B3LYP/ 6-311++(2d,2p)	MP2/ 6-311++G(2d,2p)	MM3	MM4
E(uncorrected)		-3.38	-4.01		
BSSE		-0.13	-0.40		
E(corrected)		-3.25	-3.61	-3.47	-3.83
Dipole Moment		0.000	0.000	0.000	0.000
Imaginary Fre.		3	3	1	2
O...O dist.		2.800	2.781	2.832	2.736
O...H dist.		2.318	2.299	2.300	2.213
<H-O...O		51.0	50.9	47.5	48.4

III. (H ₂ O) ₂ (bifurcated, C _{2v}), 4					
		B3LYP/ 6-311++(2d,2p)	MP2/ 6-311++G(2d,2p)	MM3	MM4
E(uncorrected)		-2.96	-3.44		
BSSE		-0.19	-0.44		
E(corrected)		-2.77	-2.99	-4.36	-3.88
Dipole Moment		4.228	4.443	4.163	3.863
Imaginary Fre.		1	1	1	1
O...O dist.		3.031	3.016	2.746	2.733
O...H dist.		2.542	2.522	2.266	2.256
<H-O...O		51.2	50.8	50.6	51.2

^a Experimental geometry is microwave r_0 structure; MM3 and MM4 geometries are r_g values. QM values are approximate r_e values (as calculated without correction); energies are in kcal/mol; distances are in Å; angles are in deg. ^b O...X is the bisector of the angle H-O-H (see Figure 3). ^c Reference 34a. ^d Reference 34b. ^e Reference 35. ^f CCSD(T) limit (ref 35).

findings are consistent with the idea that the position of the lone-pair (rather than just the oxygen) plays an important role in force field calculations of hydrogen bonding.

Because ordinary hydrogen bonding occurs from the interaction of the hydrogen with a lone-pair of electrons, and not with the heteroatom nucleus, it was believed that a better model would include the “position” of the lone-pair that is hydrogen bonded.^{27,28} Various schemes were investigated, wherein the lone-pair was assigned van der Waals and electrostatic properties as in the old MM2 program. While workable, this procedure led to a number of additional complications, and it was subsequently decided that the “position” could better be represented by just an orientation, the lone-pair directionality.

This additional term was therefore introduced into MM4(98)^{29,30} (eq 3 and Figure 4) to improve the calculation of hydrogen-bonding geometries, and especially to improve conformational energies when intramolecular hydrogen-bonding interactions are involved, as in ethylene glycol.

$$E_{\text{HB}} = \sum \varepsilon_{\text{HB}} \{ 276\,000 \exp[-12.0R_{\text{HB}}/R_{\text{HB}}^{\circ}] - F(\theta_{\text{H-A-B}}, \theta_{\text{H-B-LP}}, l_{\text{AH}}) 2.25(R_{\text{HB}}^{\circ}/R_{\text{HB}})^6 \} \quad (3)$$

where $F(\theta_{\text{H-A-B}}, \theta_{\text{H-B-LP}}, l_{\text{AH}})$ means a function of the indicated variables, and LP means the lone-pair (or equivalent) of electrons, and specifically:

$$F(\theta_{\text{H-A-B}}, \theta_{\text{H-B-LP}}, I_{\text{AH}}) = N[\cos(\theta_{\text{H-A-B}}) + 1]^n [\cos(\theta_{\text{H-B-LP}}) + 1]^n (I_{\text{AH}}/I_{\text{AH}}^0)$$

and the normalization factor N is introduced so that the product of $[\cos(\theta_{\text{H-A-B}}) + 1]^n$ and $[\cos(\theta_{\text{H-B-LP}}) + 1]^n$ will lie between 0 and 1. For the case of nitrogen, $N = 1/4$ and $n = 1$. For the case of oxygen or halogens, $N = 1/16$ and $n = 2$. Note that the dielectric constant is no longer involved in the MM4 hydrogen-bonding formulation. The term removed from the previous formulation (MM3, eq 2, Figure 2) is based on the information from Table 2. The attractive term in eq 3 should be mainly from the charge transfer, and because this is formally bonding, we have taken it to be dielectric constant independent. The directionality of the vector representing the lone-pair in Figure 4 is determined by the angle ϕ , which is the angle between the lone-pair and the reference axis. In the case where the B atom is bound to only one atom X, the reference axis is the B–X bond itself. If B is bound to two or more atoms, such as BXY or BXYZ, the reference axis is the line that connects atom B to the midpoint of line X···Y or the centroid of the plane XYZ. The ϕ value is set according to the atom type of B. It is 70° for oxygen (whether it is a carbonyl, alcohol, ether, or water oxygen), 65° for a halogen atom, and 0° for amine nitrogen atom. The result of this way of defining the lone-pair directionality in eq 3 is that, in the oxygen case, the hydrogen-bond interaction around the reference axis is the same (no specific location of lone-pair is given). Any differences in the resulting hydrogen-bond geometry will result from steric and electrostatic effects of the attached atoms.

Computational Method

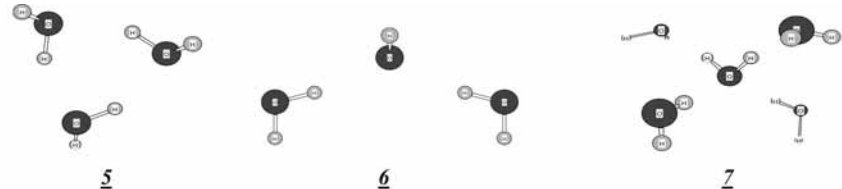
Quantum mechanical (QM) calculations with the 6-311++G(2d,2p) basis set at the MP2 and B3LYP levels of theory using the Gaussian³¹ program were carried out for all dimers and

conformations as below unless otherwise stated. For convenience, these calculations will be referred to as MP2/B and DFT/B calculations through this paper. (The symbol B is used to represent the indicated basis set, referred to locally as “Big.”) Counterpoise Basis Set Superposition Error (BSSE) corrections³² were also used for all dimers, trimers, and the pentamer. In MM4 calculations, the vectors that account for the lone-pair directionality are implicitly placed along the lines defined by the hydrogen acceptors and their chemically intuitive electron pairs. No lone-pairs are actually used in the calculations. Instead, the H-bond angularity function, $[\cos(\theta_{\text{H-A-B}}) + 1]^n$, and the lone-pair directionality function, $[\cos(\theta_{\text{H-B-LP}}) + 1]^n$, are used.

The MM4 hydrogen-bonding parameters were then optimized to fit the ab initio results, and the experimental values when they were available. The discussion of the overall results calculated with optimized parameters (shown in Table 3) as compared to the ab initio and the experimental results follows (Tables 4–11).

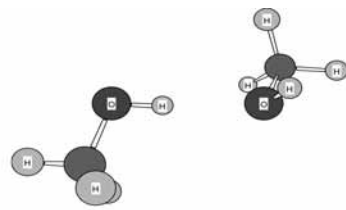
The hydrogen bonding in MM4 is accounted for automatically by the program. It only requires that a hydrogen and an electron pair donor be located near one another in space. Only two parameters are required to define the hydrogen bond. These parameters are characteristic of the pair of atom type numbers involved. They replace the two corresponding van der Waals parameters (ϵ and R°) in the calculation for that specific pair of atoms. In this Article, we discuss only water, alcohols, and hydrogen fluoride, each of which requires a separate parameter set. Invariably the parameters are such that they deepen the potential well and move the minimum to shorter distance. In most cases, the majority of the hydrogen-bond energy comes from the electrostatics, and the way that it is calculated is not changed. (The numerical value typically is increased, however, as the distance between dipoles decreases. The changes brought about by these parameters include the changes in quantities that

TABLE 6: Geometries and Energies of Water Trimers and Pentamer



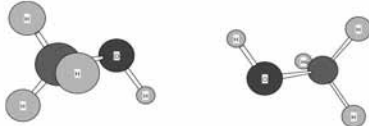
	O...O distance (Å) ^a					
	Exp. ^b	MP2/ aug-cc-pVQZ ^c	B3LYP/ 6-311++G(2d,2p)	MP2/ 6-311++G(2d,2p)	MM3	MM4
Trimer (cyclic), <u>5</u>	2.86-2.87	2.779 2.782 2.784	2.807 2.807 2.816	2.804 2.806 2.813	2.934 2.936 2.936	2.888 2.892 2.901
Trimer (chair), <u>6</u>			2.951 2.951	2.947 2.947	2.959 2.959	2.961 2.961
Pentamer, <u>7</u>			2.832 2.832 2.854 2.854	2.824 2.824 2.845 2.845	2.942 2.942 2.944 2.944	2.943 2.943 2.945 2.945
		E (kcal/mol) / Dipole Moment (Debye)				
		MP2 Limit ^c	B3LYP/ 6-311++G(2d,2p) ^d	MP2/ 6-311++G(2d,2p) ^d	MM3	MM4
Trimer (cyclic), <u>5</u>		-15.82(5)	-14.71 / 1.189	-14.33 / 1.169	-12.25 / 0.093	-12.68 / 0.957
Trimer (chair), <u>6</u>			-8.07 / 0.255	-7.96 / 0.012	-8.71 / 1.903	-8.76 / 0.270
Pentamer, <u>7</u>			-22.04 / 0.396	-21.43 / 0.544	-19.3 / 3.394	-19.18 / 0.524

^a Both MM3 and MM4 values are r_g values. Trimer (5) and pentamer (6) have been restricted to C_{2v} symmetry. ^b Reference 36. ^c Reference 37. ^d BSSE corrected binding energies.

TABLE 7: Geometries and Energies of Methanol Dimers^a


I

	CCSD(T) Limit	B3LYP/ 6-311++G(2d,2p)	MP2/ 6-311++G(2d,2p)	MM3	MM4
I. (CH₃OH)₂ (linear, C₁), I					
E(uncorrected)		-5.07	-6.25		
BSSE		-0.31	-1.06		
E(corrected)	-5.45 ^c -5.70 ^d	-4.76	-5.19	-4.87	-5.45
Dipole Moment		2.819	2.800	3.112	2.794
Imaginary Fre.		0	0	0	0
O...O dist.		2.893	2.851	2.957	2.902
O...H dist.		1.927	1.895	2.004	1.936
<O...O-H		3.7	6.6	2.4	4.0
<O...O...X ^b		129.1	123.3	155.4	126.6



II

	B3LYP/ 6-311++G(2d,2p)	MP2/ 6-311++G(2d,2p)	MM3	MM4
II. (CH₃OH)₂ (cyclic, C_{2h}), II				
E(uncorrected)	-4.01	-4.99		
BSSE	-0.22	-0.75		
E(corrected)	-3.79	-4.24	-3.41	-3.18
Dipole Moment	0.013	0.009	0.000	0.000
Imaginary Fre.	3	3	3	2
O...O dist.	2.828	2.789	2.791	2.689
O...H dist.	2.274	2.240	2.306	2.250
<O...O-H	46.4	46.6	50.5	53.4

^a Both MM3 and MM4 geometries are r_g values. Energies are in kcal/mol; distances are in Å; angles are in deg. ^b O...X is the bisector of the angle C–O–H (see Figure 3). ^c Reference 38. ^d Reference 39.


are additional to the electrostatics. In quantum mechanics, these are taken to include mainly charge transfer, dispersion, and polarization. In MM4, dispersion is normally included in the van der Waals attraction anyway, and polarization energy (induced dipole) is calculated separately and added. Thus, the MM4 hydrogen-bond model is consistent with what we know from quantum mechanics and is implemented with the aid of just two parameters, which are atom type dependent. Note that the hydrogen bond from water to water, and that from methanol to methanol, have energy parameters (ϵ) that differ by about 1 kcal/mol.)

Results and Discussion

Hydrogen Fluoride Dimer. Because quantum mechanics tells us that hydrogen bonds are mainly electrostatic in nature, one might have expected that the HF dimer would have the two molecules side by side in an antiparallel geometry. However, that is not what is found. If the hydrogen bond were strong enough to overcome the electrostatics (dipole–dipole), then one might expect to find a linear dimer (with F...F–H 180°), because this geometry can yield a reasonably good arrangement for both of the dipoles (head-to-tail) with the

hydrogen bond linear. This was what MM3 calculated. However, both experiment^{33a} and the best quantum mechanical calculations^{33c,d} show that the hydrogen fluoride dimer has neither the linear nor the parallel geometry that might have been expected. Instead, the (HF)₂ dimer **1** is “V” shaped (see graphic in Table 4). All four atoms are in the same plane, with F...F–H angles of 117° and 112°, respectively (Table 4). With the inclusion of lone-pair directionality, the MM4 value (124.8°) is now in reasonable agreement with both the experimental and the ab initio results (Table 4 and Figure 5). The binding energies are 4–7 kcal/mol experimentally,^{33b} 3.9–4.4 by quantum mechanics, and 4.6 by MM4.

Water Dimers, Trimers, and Pentamer. There were three water dimers, two trimers, and an ice-like pentamer included in this study. An ab initio study of these six water clusters with full geometry optimizations and including BSSE corrections was carried out. The MM4 hydrogen-bonding potential for O–H...O (type 6–180...6) was then optimized to fit to the ab initio structures and binding energies. Table 5 clearly shows that the MM4 hydrogen-bonding potential with the inclusion of lone-pair directionality gives a significant improvement in the dimer geometry, relative to earlier calculations. Unlike MM3, which

TABLE 8: Summary of Experiment and Calculation Results for Methanol–Water (MW) and Water–Methanol (WM) Dimers^a


	Method	Parameters	MW, <u>10</u>	WM, <u>11</u>	Ref.		
Geometries	Microwave	O...O	-	2.997	40		
		MP2/6-311++G(2d,2p)	O...O	2.912	2.857	This work	
	MM3	O...O...X ^b	128.1	117.3	"		
		O...O	2.947	2.954	"		
		O...O...X	166.8	148.7	"		
MM4	O...O	2.885	2.965	"			
	O...O...X	128.9	122.1	"			
Moments of Inertia	Microwave ^c	I_a	-	2.9692	40		
		I_b	-	19.8293	"		
		I_c	-	22.3968	"		
	MM3	I_a	2.8021	2.6273	This work		
		I_b	21.9854	22.7941	"		
		I_c	23.8564	24.5504	"		
	MM4 ^c	I_a	2.5111	3.0713	"		
		I_b	21.4063	20.5291	"		
		I_c	23.0141	22.5397	"		
Dipole Moment	Microwave	μ	-	2.625	40		
		MP2/6-311++G(2d,2p)	μ	2.917	2.554	This work	
	MM3	μ	3.389	3.152	"		
		MM4	μ	2.735	2.563	"	
	Binding Energies	Method	Parameters	MW, <u>10</u>	WM, <u>11</u>	Ref.	
LCAO-SCF/STO-3G				ΔE	-6.260	-5.220	41a
HF/6-31G*				ΔE	-5.550	-5.730	41b
HF/6-31G				ΔE	-6.740	-7.780	41c
MP2/CBSB3 ^d				ΔE	-5.500	-5.900	41d
MP4/CBSB4 ^e				ΔE	-5.700	-5.900	41d
B3LYP/6-311++G(2d,2p) ^f				ΔE	-4.386	-4.978	This work
MP2/6-311++G(2d,2p) ^f				ΔE	-4.453	-5.150	"
MM3				ΔE	-5.042	-4.525	"
MM4				ΔE	-4.394	-5.102	"

^a Distances in Å; angles in deg; moments of inertia in unit of 10^{-39} g cm²; dipole moments in Debye; energies in kcal/mol. ^b O...X is the bisector of the angle H–O–H in dimer **10** and C–O–H in dimer **11** (see Figure 3). ^c Experiment and MM4 moments of inertia are r_z values, and MM3 moments of inertia are r_g values. ^d Computed on MP2/6-31G(d). ^e Computed on MP2/6-31G(d'). ^f With BSSE correction.

TABLE 9: Methanol/Water Dimer Energies (kcal/mol)^a

dimers	MP2/B	MM4	
H ₂ O/H ₂ O	2	-4.61	-4.59
MeOH/MeOH	8	-5.19	-5.45
MeOH...OH ₂	10	-4.45	-4.39
HOH...O(H)Me	11	-5.15	-5.10

^a Relative to the two separate fragments.

predicted the O1...O2...X (O2...X is the bisector of H₂–O₂–H₂ angle, Figure 3) angle of the linear water dimer **2** to be 160.3°, MM4 now calculates the angle to be 123°, which is very close to both the ab initio and the experimental^{34a} results (122.5°,³⁵ 123.7°, and 123°(10), respectively). Simultaneously, the dipole moment of the dimer is also improved, due to the improvement of the dimer geometry.

Other water dimers appear to be possible, and we have examined two of them, which will be referred to as cyclic **3** and bifurcated **4**. Their important properties are given in Table

5. Geometries were found in both cases that correspond to stationary points, but not to energy minima. (Both have imaginary vibrational frequencies.) They have energies about 1 kcal/mol above that of **2**. The MM4 structures and energies for the cyclic **3** and bifurcated **4** water dimers do not change much from the MM3 values. Further studies of the water trimers **5**, **6** and the pentamer **7** with MM4 also show some improvement (Table 6). The MM4 O...O distances in all of the trimers and the pentamer are in fair agreement with QM results. Although the binding energies of those trimers and pentamer are also slightly improved from MM3 results,²³ MM4 still somewhat underestimates (as compared to DFT/B and MP2/B results) the binding energy of the cyclic trimer **6** and the pentamer **7**. (When MM4 was originally developed (mid-1990s), polarization was not included. Later it became clear that this really needed to be added, if one wanted to obtain chemical accuracy in a general way in the results.⁴⁵ We had already done a lot of development of MM4 without this term and could not

TABLE 10: Conformational Energies and Dipole Moments of Ethylene Glycol

conformations ^a	E_{rel} (kcal/mol)/dipole (Debye)			
	B3LYP/6-311++	MP2/6-311++	MM3	MM4
	G(2d,2p)	G(2d,2p)		
tGg', 12	0.00/2.463	0.00/2.731	0.00/2.660	0.00/2.763
gGg', 13	0.33/2.458	0.55/2.687	0.98/2.622	0.56/2.424
g'Gg', 14	0.84/0.149	1.14/0.309	NA ^b	0.97/0.781
gTg', 15	2.45/0.006	2.92/0.000	3.40/0.000	3.96/0.000
tTt, 16	2.46/0.001	2.66/0.001	2.04/0.000	2.27/0.000
tTg, 17	2.52/2.141	2.86/2.307	2.93/2.269	3.33/2.399
gTg, 18	2.67/2.483	3.13/2.609	3.98/3.111	4.24/2.762
gGg, 19	2.80/1.671	3.28/1.820	NA ^b	2.45/1.408
tGt, 20	2.95/1.311	3.21/1.680	2.62/1.449	2.99/0.871
tGg, 21	3.36/3.285	3.78/3.573	3.62/3.374	3.16/3.187
TS1, 22^c	4.70/1.818	5.65/1.986	5.81 ^d /1.884	5.82 ^d /2.006
TS2, 23^e	6.19/3.435	6.96/3.700	6.97 ^d /3.189	6.50 ^e /3.326

^a The three dihedral angles are H1–O1–C–C, O1–C–C–O2, and C–C–O2–H2, respectively; g,G, gauche(+); g',G', gauche(-); t,T, trans (see Figure 5). ^b Stable conformation could not be found on the MM3 potential surface. ^c TS1 (with O–C–C–H eclipsed) and TS2 (with O–C–C–O eclipsed) are rotational transition states (see Figure 5). ^d One imaginary frequency in MM3 and MM4. ^e Two imaginary frequencies in MM4.

really justify going back and redoing it all again with the polarization included properly in the energy minimization. So what we did was to add the polarization energy as a single point calculation, to correct the energies of the structure obtained without polarization. This is in general much better than just leaving out the polarization entirely. On the other hand, in some cases it is not very satisfactory. In this particular case, the energy surface is fairly flat, and the polarization tends to compact the molecule. When the geometry is optimized without polarization, the molecule is too large, and things are too far apart. The calculated polarization energy is also too small. If the geometry were optimized, the molecule would compact, and the polarization energy would increase, stabilizing the system. So part of the error in the energies of the water trimer and pentamer is believed to be due to the inaccuracy of the calculation of these polarization energies.) The MM4 dipole moments for trimers and the pentamer are significantly improved (Table 6). The results show that the MM4 structures, especially the orientation of hydrogens, for these water clusters are in somewhat better agreement with the ab initio results than were the earlier molecular mechanics results.

Methanol Dimers and Water–Methanol Dimers. The methanol dimers **8**, **9** lie on a more simple potential surface than do the water dimers, because there is only one hydrogen per molecule that can form a hydrogen bond. The MM4 results show significant improvements in both geometries and binding energies for methanol dimer (see Table 7). In particular, the O1···O2···X (O2···X is the bisector of the C2–O2–H2 angle, Figure 3) angle and the dipole moment of the linear methanol dimer, **8**, are improved significantly. They are calculated to be 126.6° and 2.79 Debye by MM4, respectively, while the MP2/B calculation gives values of 123.3° and 2.80 Debye. MM3 gave 155.4° and 3.11 Debye.

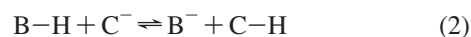
The MM4 geometries and binding energies for the water–methanol dimer **10** (MW, methanol as proton donor) and **11** (WM, water as proton donor) are also improved from the MM3 results (Table 8). Just like linear water dimer and methanol dimer, the O1···O2···X angles (O2···X is the bisector of the H2–O2–H2 and the C2–O2–H2 angle in water and methanol, respectively, Figure 3) are significantly improved. They are

calculated to be 128.9° and 122.1° for dimer **10** and **11** by MM4, respectively. The MP2/B gives values of 128.1° and 117.3°, and MM3 gives 166.8° and 148.7°, respectively. As compared to the microwave results,⁴⁰ the moments of inertia and dipole moments are also improved due to the better O1···O2···X angle, especially for dimer **11**. Table 8 shows the MM4 binding energies for dimer **10** and dimer **11** are in good agreement with MP2/B results.⁴¹

Methanol/Water Dimer Energies. The relative acidities of water, methanol, and *t*-butyl alcohol have long been of interest. The older literature states that water is the most acidic, and *t*-butyl alcohol the least. This is certainly found to be true in the homogeneous liquids. However, as was shown by Brauman,⁴² the reverse is true in the gas phase. While we might think of acidity as being measured by reaction 1:



such reactions are extremely endothermic (about 300 kcal/mol for a strong acid-like HCl) and really do not occur in the gas phase. Yet what we can look at in the gas phase are reactions of type 2.



This type of reaction is exothermic if B–H is more acidic, or if C⁻ is more basic, by a dominating amount. We usually think in terms of acidities. Hence, for hydrogen-bond formation, we might expect a stronger hydrogen bond in the order *t*-butyl > methanol > water in the gas phase. In Table 9 are given the relative energies for various dimers, calculated by MP2/B, and also by MM4.

First, note that the MM4 values agree well with the MP2/B values, the largest discrepancy being only 0.20 kcal/mol. The methanol dimer **8** is indeed more stable than the water dimer **2**, 5.19 versus 4.61 kcal/mol by MP2/B, as expected. Yet when we look at the mixed dimers, the results are less straightforward. When the more acidic methanol hydrogen bonds to water **10**, the dimer bonding energy is less than when the less acidic water bonds to methanol **11**. Note that in fact the more stable dimers have methanol bonded to methanol, or water bonded to methanol. The less stable ones have methanol bonded to water, or water bonded to water. It makes essentially no difference which of the two monomers is acting as the hydrogen donor. What is important in determining the dimer energy is which molecule is acting as the hydrogen acceptor. This is certainly not what we would have anticipated and clearly will be worth further study. However, for present purposes, we note that when the hydrogen bonds from water and methanol are given appropriate MM4 parameters so as to fit the energies from MP2/B calculations, the mixed dimers come out with the correct energies automatically. When we compare term by term the 20 numbers that constitute the MM4 total steric energy of **10** with that of **11**, the latter is lower by 0.81 kcal/mol, and this difference comes almost completely from the hydrogen-bond term (0.89 kcal/mol) resulting from the parameters in Table 3. Thus, it is not from simple electrostatics in MM4, but it is from the van der Waals term (which includes charge transfer).

Ethylene Glycol. Ethylene glycol contains a key moiety (O–C–C–O) required for modeling studies of carbohydrates. It is important to get the ethylene glycol potential surface right so that one can transfer the alcohol/ether parameters to carbohydrate calculations. Also, the ethylene glycol potential surface is dependent on the hydrogen-bond interaction between the two vicinal hydroxyl groups. Twelve conformations of ethylene glycol were studied (Table 10, Figure 6). They are 10

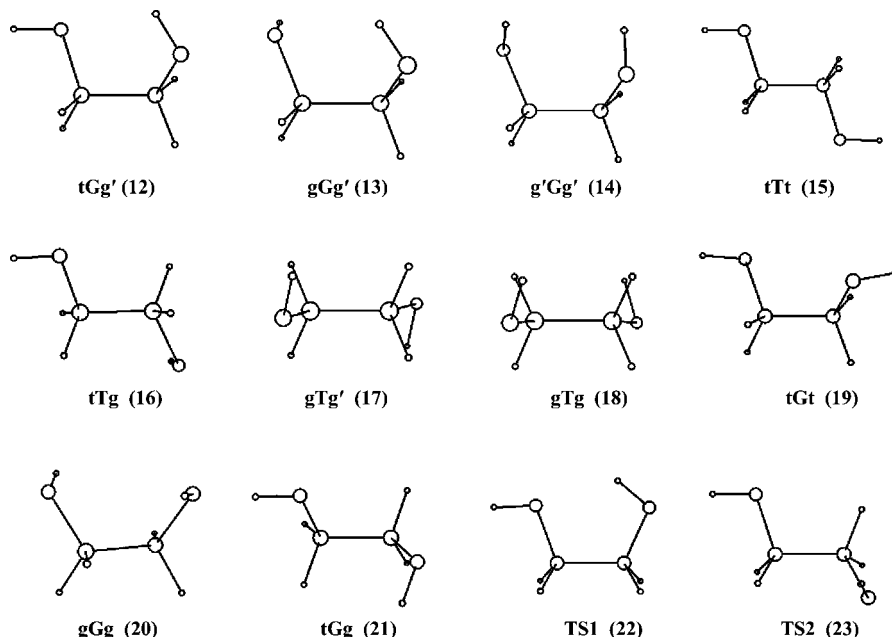
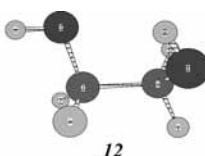


Figure 6. Conformations of ethylene glycol.

TABLE 11: Geometry and Energy of Ethylene Glycol (tGg')^a


	R_c			R_g	
	MP2/ 6-311++G(2d,2p)	MM3	MM4	E.D ^b	MM4
E(tTt)-E(tGg')	2.66	2.04	2.27		
C1-C2	1.508	1.514	1.507	1.517	1.514
C1-O3 (H acceptor)	1.434	1.426	1.424	1.424 _{ave}	1.430
C2-O4	1.422	1.424	1.421		1.427
O3-H5	0.958	0.930	0.952	0.961 _{ave}	0.967
O4-H6 (H donor)	0.962	0.932	0.955		0.97
C2-C1-O3	105.9	108.2	107.1	} 109.3 (4) _{ave}	109.5 _{ave}
C1-C2-O4	111.2	109.2	111.2		
C1-O3-H5 (H acceptor)	108.8	108.2	108.7	} 105.8 (27) _{ave}	106.9 _{ave}
C2-O4-H6 (H donor)	106.0	106.2	106.4		
H6-O4-C2-C1	-167.3	179.5	179.2		
O3-C2-C1-O4	62.0	61.7	62.9	60.7 (18)	63.2
C2-C1-O3-H5	-51.8	-50.5	-48.2		

^a The r_g structure by ED is at 376 K. ^b Reference 39.

stable conformers and 2 rotational transition states as shown in Table 10. As one can see from the table, the MM4 results are comparable to those from MP2/B theory. It is particularly important that the low energy conformations have their energies well calculated, as they will correspond, for the most part, to the conformations that will actually be most often found in more complex systems. The three lowest energy conformations are, in increasing order, **12**, **13**, and **14**, by MP2/B (and also by DFT/B), and the MM4 values are within about 0.2 kcal/mol of the MP2/B values in each case. The high energy conformations are generally fairly well calculated, but there are two errors of about 1.3 kcal/mol.

Conformations **12**, **13**, and **14** can internally hydrogen bond, with a favorable XGg' arrangement. This arrangement between the oxygens and the hydrogen that forms the hydrogen bond is optimum and is lacking in all other conformations. These

conformations have MM4 hydrogen bonds that range in strength (electrostatics, van der Waals, and induced dipole) of -1.74 , -0.91 , -0.37 kcal/mol, for **12**, **13**, and **14**, respectively, which is sufficient to lower their stabilities by at least 1 kcal/mol below the remaining conformations.

The MM4 geometry of the most stable conformation (tGg', **12**) was compared to the experimental electron diffraction structure (r_g)⁴³ and with the MP2/B calculation (r_c) (Table 11). Some important values cannot be uniquely determined from the diffraction pattern and are only reported as average values with similar quantities. The agreement is satisfactory. The MP2/B values can be compared to MM4 item by item. One significant improvement in the MM4 results over those of MM3 is that conformer g'Gg' **14**, which is found from all QM calculations but not found as a stationary point from the MM3 results, is now found by the MM4 calculation as well. This difference

appears to be due to the inclusion of lone-pair directionality in the MM4 hydrogen-bonding potential.

Summary

Continuing studies showed that the MM3 treatment of the hydrogen bond still proved to be inadequate in some cases, and at least one more item needed to be accounted for in the molecular mechanics treatment. This remaining item concerned the lone-pair that was the proton acceptor of the hydrogen bond. Most earlier calculations generally ignored the fact that the lone-pair had an average position that was out away from the nucleus to which it was attached. Some early calculations⁴⁴ had approximated the lone-pair on nitrogen (for an amino group) as having an average distance of 0.60 Å from the nitrogen, and along the amino group symmetry axis (for a symmetrical amine or ammonia). This offset becomes important in cases such as ethylene glycol, where one hydroxyl wants to point, not just toward the other oxygen (nucleus), but specifically toward a lone-pair attached to that oxygen.

In the present work, we confirmed the importance of explicitly accounting for lone-pair electrons in force field calculations on hydrogen bonding and proposed a new hydrogen-bonding model, which is included in the MM4(98) and subsequent force fields.³⁰ The inclusion of the lone-pair directionality results in improved accuracy in hydrogen-bonded geometries, interaction energies (such as the dimers of hydrogen fluoride, water, methanol, and water–methanol), and especially the conformational energies when intramolecular hydrogen-bonding interactions are involved, as in ethylene glycol.

References and Notes

- (1) Jeffrey, G. A.; Saenger, W. *Hydrogen Bonding in Biological Structure*; Springer-Verlag: Berlin/New York, 1991.
- (2) Watson, J. D.; Crick, F. H. C. *Nature* **1953**, *171*, 737.
- (3) Pauling, L.; Corey, R. B.; Branson, H. R. *Proc. Natl. Acad. Sci. U.S.A.* **1951**, *37*, 205.
- (4) (a) Pauling, L. *J. Am. Chem. Soc.* **1931**, *53*, 1367. (b) Pauling, L. *The Nature of the Chemical Bond*; Cornell University Press: Ithaca, NY, 1939. (c) Pimentel, G. C.; McClellan, A. L. *The Hydrogen Bond*; Freeman: San Francisco, CA, 1960. (d) Jeffrey, G. A. *An Introduction to Hydrogen Bonding*; Oxford University Press: Oxford, 1997.
- (5) Gordy, W.; Stanford, S. C. *J. Chem. Phys.* **1940**, *8*, 170.
- (6) Hammett, L. P. *J. Chem. Educ.* **1940**, *17*, 131.
- (7) Stanford, S. C.; Gordy, W. *J. Am. Chem. Soc.* **1941**, *63*, 1094.
- (8) Curran, C. *J. Am. Chem. Soc.* **1945**, *67*, 1835.
- (9) Latimer, N. M.; Rodebush, W. H. *J. Am. Chem. Soc.* **1920**, *42*, 1419.
- (10) (a) Kasha, M. *Discuss. Faraday Soc.* **1950**, *9*, 14. (b) Olovsson, I.; Jonsson, P. G. *Hydrogen Bond* **1976**, *2*, 393. (c) Olovsson, I. *Z. Phys. Chem.* **2006**, *220*, 963. (d) Newton, M. D.; Jeffrey, G. A.; Takagi, S. *J. Am. Chem. Soc.* **1979**, *101*, 1997.
- (11) Lennard-Jones, J.; Pople, J. A. *Proc. R. Soc.* **1951**, *A205*, 155.
- (12) Pople, J. A. *Proc. R. Soc.* **1957**, *A239*, 541, 550.
- (13) Kollman, P. A.; Allen, L. C. *Theor. Chim. Acta* **1970**, *18*, 399.
- (14) Dreyfus, M.; Pullman, A. *Theor. Chim. Acta* **1970**, *19*, 20.
- (15) Morokuma, K. *J. Chem. Phys.* **1971**, *55*, 1236.
- (16) Coulson, C. A. *Research (London)* **1957**, *10*, 149.
- (17) Umeyama, H.; Morokuma, K. *J. Am. Chem. Soc.* **1977**, *99*, 1316.
- (18) Morokuma, K.; Winick, J. R. *J. Chem. Phys.* **1970**, *52*, 1301.
- (19) Allinger, N. L. *J. Am. Chem. Soc.* **1977**, *99*, 8127.
- (20) Burkert, U.; Allinger, N. L. *Molecular Mechanics*; American Chemical Society: Washington, DC, 1982.
- (21) Allinger, N. L.; Kok, R. A.; Imam, M. R. *J. Comput. Chem.* **1988**, *9*, 591.
- (22) (a) Allinger, N. L.; Yuh, Y. H.; Lii, J.-H. *J. Am. Chem. Soc.* **1989**, *111*, 8551. (b) The MM3 program is available from: Allinger, N. L. Department of Chemistry, University of Georgia, Athens, GA 30602.
- (23) Lii, J.-H.; Allinger, N. L. *J. Phys. Org. Chem.* **1994**, *7*, 591.
- (24) Lii, J.-H.; Allinger, N. L. *J. Comput. Chem.* **1998**, *2*, 1271.
- (25) Hehre, W. J.; Radom, L.; Schleyer, P. v. R.; Pople, J. *Ab Initio Molecular Orbital Theory*; John Wiley and Sons: New York, 1986; p 324.
- (26) Chen, K.-H.; Lii, J.-H.; Fan, Y.; Allinger, N. L. *J. Comput. Chem.* **2007**, *28*, 2391.
- (27) (a) Allinger, N. L.; Chung, D. Y. *J. Am. Chem. Soc.* **1976**, *98*, 6798. (b) Brooks, B. R.; Bruccoleri, R. E.; Olafson, B. D.; Strates, D. J.; Swaminathan, S.; Karplus, M. *J. Comput. Chem.* **1983**, *4*, 187.
- (28) Lii, J.-H. Hydrogen Bonding: 2. In *The Encyclopedia of Computational Chemistry*; Schleyer, P. v. R.; Allinger, N. L.; Clark, T.; Gasteiger, J.; Kollman, P. A.; Schaefer, H. F., III.; Schreiner, P. R., Eds.; John Wiley & Sons: Chichester, 1998; p 1271.
- (29) Allinger, N. L.; Chen, K.; Lii, J.-H. *J. Comput. Chem.* **1996**, *17*, 642. (a) The MM4 program is available from Allinger, N. L. Department of Chemistry, University of Georgia, Athens, GA 30602. (b) Allinger, N. L.; Chen, K.-H.; Lii, J.-H.; Durkin, K. A. *J. Comput. Chem.* **2003**, *24*, 1447. (c) Lii, J.-H.; Chen, K.-H.; Durkin, K. A.; Allinger, N. L. *J. Comput. Chem.* **2003**, *24*, 1473. (d) Lii, J.-H.; Chen, K.-H.; Grindley, T. B.; Allinger, N. L. *J. Comput. Chem.* **2003**, *24*, 1490. (e) Lii, J.-H.; Chen, K.-H.; Allinger, N. L. *J. Comput. Chem.* **2003**, *24*, 1504. (f) Lii, J.-H.; Chen, K.-H.; Allinger, N. L. *J. Phys. Chem. A* **2003**, *108*, 3006.
- (30) Langley, C.; Allinger, N. L. *J. Phys. Chem. A* **2003**, *107*, 5208.
- (31) Frisch, M. J.; Trucks, G. W.; Schlegel, H. B.; Gill, P. M. W.; Johnson, B. G.; Robb, M. A.; Cheeseman, J. R.; Keith, T. A.; Peterson, G. A.; Montgomery, J. A.; Raghavachari, K.; Al-Laham, M. A.; Zakrewski, V. G.; Ortiz, J. V.; Foresman, J. B.; Cioslowski, J.; Stefanov, B. B.; Nanayakkara, A.; Challacombe, M.; Peng, C. Y.; Ayala, P. Y.; Chen, W.; Wong, M. W.; Andres, J. L.; Replogle, E. S.; Gomperts, R.; Martin, R. L.; Fox, D. J.; Binkley, J. S.; Defrees, D. J.; Baker, J. P.; Stewart, J. J. P.; Head-Gordon, M.; Gonzalez, C.; Pople, J. A. *Gaussian 94*, revision E.2; Gaussian, Inc.: Pittsburgh, PA, 1995.
- (32) Boys, S. F.; Bernardi, F. *Mol. Phys.* **1970**, *19*, 553.
- (33) (a) Howard, B. J.; Dyke, T. R.; Klemperer, W. *J. Chem. Phys.* **1984**, *81*, 5417. (b) Pine, A. S.; Howard, B. J. *J. Chem. Phys.* **1986**, *84*, 590. (c) Klopfer, W.; Quack, M.; Suhm, M. A. *Chem. Phys. Lett.* **1996**, *261*, 35. (d) Klopfer, W.; Quack, M.; Suhm, M. A. *J. Chem. Phys.* **1998**, *108*, 10096.
- (34) (a) Odutola, J. A.; Dyke, T. R. *J. Chem. Phys.* **1980**, *72*, 5062. (b) Reimers, J. R.; Watts, R. O.; Klein, M. L. *Chem. Phys.* **1982**, *64*, 95.
- (35) Halkier, A.; Koch, H.; Jorgensen, P.; Christiansen, O.; Nielsen, I. M. B.; Helgaker, T. *Theor. Chem.* **1997**, *97*, 150.
- (36) Liu, K.; Cruzan, J. D.; Saykally, R. J. *Science* **1996**, *271*, 929.
- (37) Nielsen, I. M. B.; Seidl, E. T.; Janssen, C. L. *J. Chem. Phys.* **1999**, *110*, 9435.
- (38) Tsuzuki, S.; Luethi, H. P. *J. Chem. Phys.* **2001**, *114*, 3949.
- (39) Riley, K. E.; Hobza, P. *J. Phys. Chem. A* **2007**, *111*, 8257.
- (40) Stockman, P. A.; Blake, G. A.; Lovas, F. J.; Suenram, R. D. *J. Chem. Phys.* **1997**, *107*, 3782.
- (41) (a) Del Bene, J. E. *J. Chem. Phys.* **1971**, *55*, 4633. (b) Tse, Y.-C.; Newton, M. D.; Allen, L. C. *Chem. Phys. Lett.* **1980**, *75*, 350. (c) Kim, S.; Jhon, M. S.; Scheraga, H. A. *J. Phys. Chem.* **1988**, *92*, 7216. (d) Juršić, B. S. *J. Mol. Struct.* **1999**, *466*, 203.
- (42) Brauman, J. I.; Blair, L. K. *J. Am. Chem. Soc.* **1970**, *92*, 5986.
- (43) Kazerouni, M. R.; Hedberg, L.; Hedberg, K. *J. Am. Chem. Soc.* **1997**, *119*, 8324.
- (44) (a) Hermann, R. B. 1960, unpublished. This value was calculated as outlined by Coulson for the carbon case: Coulson, C. A. *Valence*; Oxford, 1952; p 207, and was used in the MM2 program. (b) Profeta, S., Jr.; Allinger, N. L. *J. Am. Chem. Soc.* **1985**, *107*, 1907.
- (45) Ma, B.; Lii, J.-H.; Allinger, N. L. *J. Comput. Chem.* **2000**, *21*, 813.